Supporting Information

Different Anions (NO$_3^-$ and OAc$^-$) Controlled Construction of Series of Dysprosium Clusters with Different Shapes

Jia-Nan Xie,[+] Yun-Lan Li,[+] Hai-Ling Wang, Zi-Xin Xiao, Zhong-Hong Zhu*, Fu-Pei Liang, and Hua-Hong Zou*

School of Chemistry and Pharmaceutical Sciences, State Key Laboratory for Chemistry and Molecular Engineering of Medicinal Resources, Guangxi Normal University, Guilin 541004, P. R. China   *E-mail   (Corresponding   author):   18317725515@163.com   (Z.-H.   Zhu), gxnuchem@foxmail.com (H.-H. Zou).

Keywords: Lanthanide clusters; Substituent and anions regulation; Solvothermal synthesis; Annular growth mechanism; Magnetic properties.

Table of Contents:

Supporting Tables	
Table S1	Crystallographic data of the clusters **1**–**3**.
Table S2	Selected bond lengths (Å) and angles (°) of clusters **1**–**3**.
Table S3	*SHAPE* analysis of the Dy(III) in cluster **1**.
Table S4	*SHAPE* analysis of the Dy(III) in cluster **2**.
Table S5	*SHAPE* analysis of the Dy(III) in cluster **3**.
Table S6	The parameters XT, XS, alpha and tau.
Note 1	SQUEEZE and "Use Solvent Mask results" results for cluster **1**–**3**.
Supporting Figures	
Figure S1	Comparison of data between the first refinement (A) and the second refinement (B).
Figure S2	Comparison of data between the first refinement (A) and the second refinement (B).
Figure S3	IR spectra of clusters **1**–**5**.
Figure S4	Thermogravimetric curves of clusters **1**–**5**.
Figure S5	Powder X-ray diffraction patterns (PXRD) of clusters **1**–**5**.
Figure S6	Temperature dependence of $\chi_m T$ for **4** and **5** (A and B).
Figure S7	M vs. H/T plots of clusters **1**–**3** (A–C).
Figure S8	M vs. H/T plots of clusters **4** and **5** (A and B).
Figure S9	Loop curve graph of clusters **1**–**3** at 2 K.
Figure S10	Temperature dependence of the real (χ') and imaginary (χ'') ac susceptibilities at different frequencies in the 0 Oe dc fields for clusters **1**–**3**.
Figure S11	Frequency-dependent χ' and χ'' curves under zero fields for clusters **1**–**3**.
Figure S12	Energy barrier fits under 0 Oe dc field for clusters **1**–**3**.

Experimental Section

Materials and Measurements.

All reagents were obtained from commercial sources and used without further purification. Elemental analyses for C, and H were performed on a varia MICRO cube. The infrared spectra were carried out on a Pekin-Elmer Two spectrophotometer with pressed KBr pellets. The X-ray powder diffraction (XRD) spectra were measured on a Rigaku D/Max-3c diffractometer with Mo Kα radiation (λ = 0.71073 Å). Thermogravimetric analyses were performed on a PerkinElmer PyrisDiamond TG-DTA instrument under an N_2 atmosphere using a heating rate of 5 °C min^{-1} from room temperature up to 1000 °C. Magnetic properties were performed on a Superconducting Quantum Interference Device (SQUID) magnetometer. The diamagnetism of all constituent atoms was corrected with Pascal's constant.

Single crystal X-ray crystallography.

Since the crystals were obviously deteriorated, the structural single crystals of compounds **1**–**3** were taken out together with the mother liquor, and then the single crystals with the mother liquor were quickly dispersed into dimethicone, and then the crystals were installed in the LOOP ring. Diffraction data for the compounds **1**–**3** was collected on a ROD, Synergy Custom DW system, HyPix diffractometer (Cu-Kα radiation and λ = 1.54 Å; and Ga-Kα radiation) in Φ and ω scan modes. The structures solved by empirical absorption correction using spherical harmonics, implemented in SCALE3 ABSPACK scaling algorithm. All the processed data were solved by SHELXT intrinsic phasing, and the refinement was done by full-matrix least squares on F^2 (SHELXL) in the Olex2 software. A solvent mask based on Platon SQUEEZE The SWAT correction was applied during the refinement for addressing the effect of diffusing solvent in the void. Anisotropic thermal parameters were applied to all non-hydrogen atoms. Hydrogen atoms were generated geometrically. The visualization of all the crystal structures was fulfilled by Olex2 as well. The crystallographic data for clusters **1**–**3** are listed in Table S1, and selected bond lengths and angles are given in Table S2. The CCDC reference numbers for the crystal structures of clusters **1**–**3** are 2291287, 2277280, and 2291288, respectively.

The structures were refined based on the following considerations. Atoms are assigned based on the results obtained by the instrument and in conjunction with the reaction materials used.

Subsequently, all non-hydrogen atoms are anisotropically generated, and hydrogen atoms are generated geometrically. Limits are imposed on individual C−C and C−N bond lengths. Especially for the terminal ends of the ligands and -CH$_3$ of the solvent molecules, there is significant disorder, resulting in atomic movement and unstable refinement. In addition, unreasonable atoms are manually modeled in idealized positions based on reasonable bond length and bond angle parameters. Model disordered benzene rings based on the initial Q peak. The last step of purification is to perform unrestricted purification of the ligand and fix the -CH$_3$ at the end of the benzene ring. The purpose of this treatment was to generate chemically reasonable models without disorder.

CheckCif alert is listed according to Alert Level B for compound complex 2

PLAT420_ALERT_2_B D-H Bond Without Acceptor O18 --H18B. Please Check

Response: The solvent molecules are highly disordered, which supposed to form hydrogen bond with water molecules, but they have been removed using the "Use Solvent Mask" command.

CheckCif alert is listed according to Alert Level B for compound complex 3

RINTA01_ALERT_3_A The value of R$_{int}$ is greater than 0.25   R$_{int}$ given   0.298

Response: The overall quality of the data was poor due to the highly sensitive and unstable nature of the compound that rendered the crystal quality low. Crystals diffracted extremely weakly and disintegrated during the data collection. Multiple attempts were made to grow better diffracting crystals, however, all this creates serious problems when mounted, as the crystal structure is sensitive to oxygen in the air and the loss of solvent molecules makes the crystal highly unstable. This resulted in weak diffraction and disorder in the solvent atom positions. In addition, due to the high degree of disorder in the benzene ring molecules in the ligand, and the obvious disorder of -CH$_3$ at the end, the atomic movement and refinement are unstable. These factors resulted in high Rint value.

PLAT020_ALERT_3_A The Value of R$_{int}$ is Greater Than 0.12 ....   0.298 Report

Response: The overall quality of the data was poor due to the highly sensitive and unstable nature of the compound that rendered the crystal quality low. Crystals diffracted extremely weakly and disintegrated during the data collection. Multiple attempts were made to grow better diffracting

crystals, however, all this creates serious problems when mounted, as the crystal structure is sensitive to oxygen in the air and the loss of solvent molecules makes the crystal highly unstable. This resulted in weak diffraction and disorder in the solvent atom positions. In addition, due to the high degree of disorder in the benzene ring molecules in the ligand, and the obvious disorder of -CH_3 at the end, the atomic movement and refinement are unstable. These factors resulted in high R_{int} value.

PLAT084_ALERT_3_A High $w\text{R}_2$ Value (i.e. > 0.25) ....   0.47 Report

Response: Generally speaking, the $w\text{R}_2$ value is about twice the R1 value. Therefore, we have done refinement of the weights and checked the model to ensure that $w\text{R}_2$ still exhibits a high value in the correct case. We believe that the quality of data is a reason that affects the $w\text{R}_2$ value. This is mainly because: The overall quality of the data was poor due to the highly sensitive and unstable nature of the compound that rendered the crystal quality low. Crystals diffracted extremely weakly and disintegrated during the data collection. Multiple attempts were made to grow better diffracting crystals, however, all this creates serious problems when mounted, as the crystal structure is sensitive to oxygen in the air and the loss of solvent molecules makes the crystal highly unstable. This resulted in weak diffraction and disorder in the solvent atom positions. In addition, due to the high degree of disorder in the benzene ring molecules in the ligand, and the obvious disorder of -CH_3 at the end, the atomic movement and refinement are unstable. These factors resulted in high $w\text{R}_2$ value. We tried using commands to remove dead pixels at high angles and using "ISOR" to constrain highly disordered atoms. But it did not reduce the value of $w\text{R}_2$. Therefore, we believe that the main reason may be due to the poor quality of the crystal itself.

[1] Sheldrick, G. M. *Acta Crystallogr., Sect. C: Struct. Chem.* **2015**, *71*, 3-8.

The synthesis method.

Synthesis of cluster 1: A mixture of 2-amino-6-methoxybenzoic acid (0.1 mmol, 16.7 mg), salicylaldehyde (0.1 mmol, 12.2 mg) and $Dy(NO_3)_3 \cdot 6H_2O$ (0.2 mmol, 90 mg) and triethylamine (30 μL) were dissolved in mixed solvent ($CH_3OH : CH_3CN = 1.2 : 0.8$) in a Pyrex tube. The tube was sealed and heated at 80 °C in an oven for 2 days, yellow crystals were observed with a yield of about 44.6% (based on $Dy(NO_3)_3 \cdot 6H_2O$). Elemental analysis theoretical value ($C_{96}H_{102}Dy_5N_{11}O_{47}$): C, 38.77%; H, 3.46%; N, 5.18%; experimental value: C, 38.65%; H, 3.31%; N, 5.01%. Infrared spectrum data (IR, KBr pellet, cm^{-1}): 3444(m), 1593(s), 1462(m), 1391(m), 1264(m), 1066(m), 755(w), 582(w).

Synthesis of cluster 2: The procedure was similar to that of cluster **1**, except that except that salicylaldehyde is replaced by 2-hydroxy-6-methoxy-benzaldehyde. The yield is about 40.5% (calculated with the amount of $Dy(NO_3)_3 \cdot 6H_2O$). Elemental analysis theoretical value ($C_{110}H_{108}Dy_8N_{16}O_{53}$): C, 34.75%; H, 2.86%; N, 5.89%; experimental value: C, 34.33%; H, 2.71%; N, 5.62%. Infrared spectrum data (IR, KBr pellet, cm^{-1}): 3409(s), 1603(s), 1456(s), 1386(s), 1071(m), 960 (m), 728(m), 597(w).

Synthesis of cluster 3: The procedure was similar to that of cluster **1**, except that except that $Dy(NO_3)_3 \cdot 6H_2O$ is replaced by $Dy(OAc)_3 \cdot 4H_2O$. The yield is about 39.6% (calculated with the amount of $Dy(OAc)_3 \cdot 4H_2O$). Elemental analysis theoretical value ($C_{215}H_{305}Dy_{14}N_{31}O_{122}$): C, 34.2%; H, 4.07%; N, 5.75%; experimental value: C, 33.91%; H, 3.89%; N, 5.59%. Infrared spectrum data (IR, KBr pellet, cm^{-1}): 3424(s), 1588(s), 1436(s), 1224(w), 1067(m), 951(w), 679(m).

Synthesis of cluster 4: The procedure was similar to that of cluster **1**. A mixture of 2-amino-6-methoxybenzoic acid (0.1 mmol, 16.7 mg), salicylaldehyde (0.1 mmol, 12.2 mg) and Gd $(NO_3)_3 \cdot 6H_2O$ (0.2 mmol, 91 mg) and triethylamine (30 μL) were dissolved in mixed solvent ($CH_3OH : CH_3CN = 1.2 : 0.8$) in a Pyrex tube. The tube was sealed and heated at 80 °C in an oven for 2 days, yellow crystals were observed with a yield of about 41.1% (calculated with the amount of $Gd(NO_3)_3 \cdot 6H_2O$). The yield is about 32.6% (calculated with the amount of $Gd(NO_3)_3 \cdot 6H_2O$). Elemental analysis theoretical value ($C_{96}H_{102}Gd_5N_{11}O_{47}$): C, 39.11%; H, 3.49%; N, 5.23%;

experimental value: C, 38.92%; H, 3.38%; N, 5.08%. Infrared spectrum data (IR, KBr pellet, cm^{-1}): 3425(s), 1592(s), 1388(s), 1268(m), 1059(m), 1066(m), 755(w), 593(w).

Synthesis of cluster 5: The procedure was similar to that of cluster **2**. A mixture of 2-amino-6-methoxybenzoic acid (0.1 mmol, 16.7 mg), 2-hydroxy-6-methoxy-benzaldehyde (0.1 mmol, 15.4 mg) and Gd (NO$_3$)$_3$·6H$_2$O (0.2 mmol, 91 mg) and triethylamine (30 μL) were dissolved in mixed solvent (CH$_3$OH : CH$_3$CN = 1.2 : 0.8) in a Pyrex tube. The yield is about 37.3% (calculated with the amount of Gd(NO$_3$)$_3$·6H$_2$O). The yield is about 35.1% (calculated with the amount of Gd(NO$_3$)$_3$·6H$_2$O). Elemental analysis theoretical value (C$_{110}$H$_{108}$Gd$_8$N$_{16}$O$_{53}$): C, 35.13%; H, 2.89%; N, 5.96%; experimental value: C, 34.89%; H, 2.75%; N, 5.79%. Infrared spectrum data (IR, KBr pellet, cm^{-1}): 3425(s), 1614(s), 1463(m), 1379(s), 1295(w), 1069(m), 739(w), 596(w).

Clusters **1**–**5** are all formed by the coordination of similar metal ions and organic ligands, so they have similar FTIR absorption peaks (Figure S3). The test results show that the broad absorption peak around 3400 cm^{-1} in the IR spectrum can be attributed to the stretching vibration of ν(HO–H) in the H$_2$O. The strong peak around 1590 cm^{-1} can be attributed to the C=N stretching vibration of the imine group. The strong peak around 1440 cm^{-1} can be attributed to the C=N and C=C stretching vibrations in the aromatic ring. The moderate-intensity absorption peak around 1100 cm^{-1} can be attributed to the stretching vibration between alcoholic hydroxyl groups C–O. The thermal stability test of clusters **1**–**5** was carried out under a flowing nitrogen atmosphere, and the temperature was slowly increased from 35 °C to 1000 °C at a rate of 3 °C min^{-1}. Before 84.5 °C, the weight loss rate of cluster **1** was 2.86%. This corresponds to the loss of five free H$_2$O (theoretical value is 3.0%). As the temperature continued to rise to 202 °C, the weight loss rate of cluster **1** was 3.14 %. This corresponds to the loss of five free molecule of H$_2$O (theoretical value is 3.12%) (Figure S4A). As the temperature continued to rise, cluster **1** was decomposed. Cluster **2** has a weight loss rate of 8.3% before 170 °C, which corresponds to the loss of six free CH$_3$CN guest molecules, one free H$_2$O, and two terminally coordinated H$_2$O (theoretical value is 7.9%). As the temperature continues to rise, cluster **2** is decomposed (Figure S4B). Cluster **3** had a weight loss of 13% before 168 °C, which corresponds to the loss of 10 free CH$_3$CN and 31 free H$_2$O (theoretical value is 12.8%). Cluster **3** was decomposed as the temperature continued to rise to 340 °C (Figure

S4C). Before 86 °C, the weight loss rate of cluster **4** was 5.0%. This corresponds to the loss of eight free H_2O (theoretical value is 4.9%). As the temperature continued to rise to 230 °C, the weight loss rate of cluster **4** was 5.3%. This corresponds to the loss of two free molecule of H_2O and two free CH_3CN (theoretical value is 4.2%) (Figure S4D). As the temperature continued to rise, cluster **4** was decomposed. Cluster **5** has a weight loss rate of 10.3% before 195 °C, which corresponds to the loss of six free CH_3CN guest molecules, one free H_2O, two terminally coordinated H_2O, and one terminally coordinated NO_3^- (theoretical value is 9.6%). As the temperature continues to rise, cluster **5** is decomposed (Figure S4E). In addition, the PXRD experimental values of clusters **1**–**5** are compared with the theoretical values (Figure S5), and the results show that they are all pure phases.

Table S1. Crystallographic data of clusters **1**–**3**.

	1	2
Formula	$C_{96}H_{102}Dy_5N_{11}O_{47}$	$C_{110}H_{108}Dy_8N_{16}O_{54}$
Formula weight	2974.3830	3802.1106
T, K	100	100
Crystal system	triclinic	monoclinic
Space group	$P\bar{1}$	$P2_1/c$
a, Å	16.3885(3)	13.39968(10)
b, Å	16.4444(4)	27.4462(2)
c, Å	20.8387(5)	16.60706(10)
α, °	101.263(7)	90
β, °	98.069(7)	93.4290(10)
γ, °	97.087(8)	90
V, Å^3	5387.2(2)	6096.66(9)
Z	2	2
D_c, g cm^{-3}	1.697	1.927
μ, mm^{-1}	18.933	26.51
$F(000)$	2678	3380
2θ range for data collection/°	5.514, 140.15	6.228, 151.46
Reflns coll.	61467	56707
Unique reflns	20117	12123
R_{int}	0.040	0.0366
Observed data [$I > 2\sigma(I)$]	20117	11624
N_{par}, N_{ref}	1330, 20117	842, 12123
$R_1{}^a$ ($I > 2\sigma(I)$)	0.0429	0.0344
$wR_2{}^b$ (all data)	0.1154	0.0866
GOF	1.044	1.067

$^aR_1=\Sigma||F_o|-|F_c||/\Sigma|F_o|$, $^bwR_2 = [\Sigma w(F_o{}^2-F_c{}^2)^2/\Sigma w(F_o{}^2)^2]^{1/2}$

	3a	3
Formula	$C_{224}H_{227}Dy_{14}N_{27}O_{107}$	$C_{215}H_{305}Dy_{14}N_{31}O_{122}$
Formula weight	7284.2773	7550.8579
T, K	100	100
Crystal system	monoclinic	monoclinic
Space group	$P2_1/n$	$P2_1/n$
a, Å	26.3873(3)	26.3873(3)
b, Å	27.8871(5)	27.8871(5)
c, Å	38.2827(5)	38.2827(5)
α, °	90	90
β, °	92.092(1)	92.092(1)
γ, °	90	90
V, Å^3	28152.1(7)	28152.1(7)

Z	4	4
D_c, g cm^{-3}	1.421	1.782
μ, mm^{-1}	19.586	19.75
$F(000)$	11536	14848
2θ range for data collection/°	4.016, 120.398	4.016, 120.398
Reflns coll.	290267	290267
Unique reflns	62206	62206
R_{int}	0.298	0.2983
Observed data [$I > 2\sigma(I)$]	41408	41408
N_{par}, N_{ref}	2532,62206	2764, 62206
R_1[a] ($I > 2\sigma(I)$)	0.1883	0.1815
wR_2[b] (all data)	0.4809	0.4694
GOF	1.743	1.695

[a]$R_1 = \Sigma||F_o|-|F_c||/\Sigma|F_o|$, [b]$wR_2 = [\Sigma w(F_o^2-F_c^2)^2/\Sigma w(F_o^2)^2]^{1/2}$
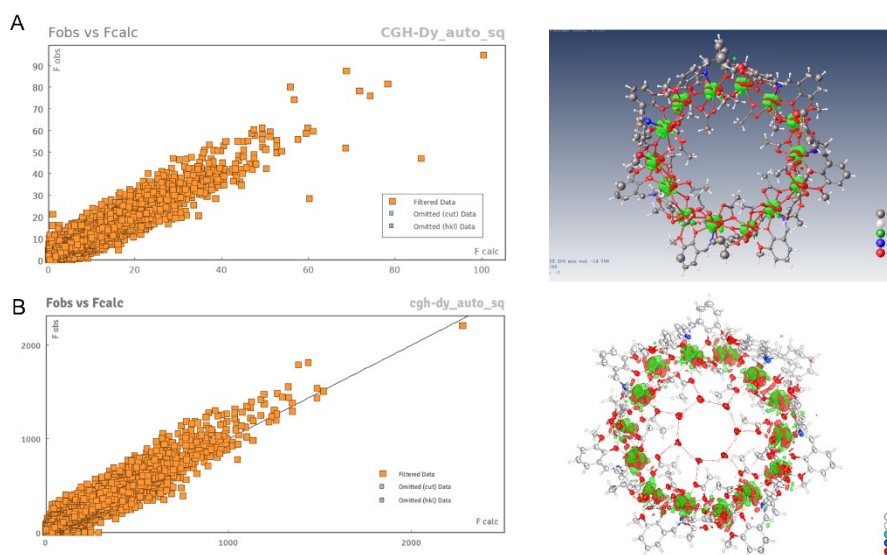
Figure S1. Comparison of data between the first refinement (A) and the second refinement (B).
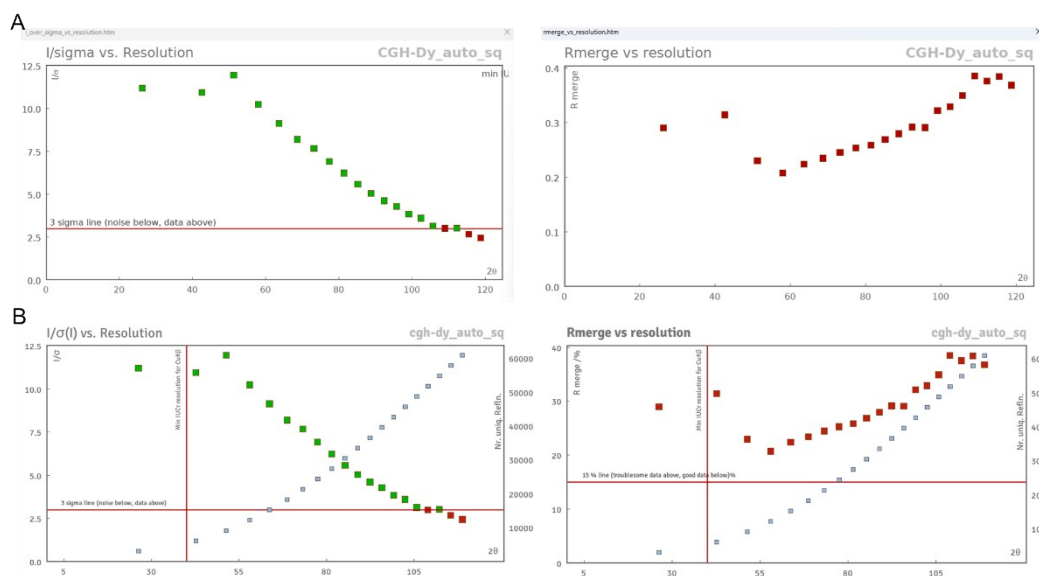
Figure S2. Comparison of data between the first refinement (A) and the second refinement (B).

Refinement of 3a (first refinement): The Solvent Mask routine of the OLEX2 software was implemented to remove the contributions of one disordered solvent to the observed structure factors. Used the SHEL 999 0.84 command to truncate some high-angle points. Atomic displacement parameter limitation commands such as ISOR, SIMU, and DELU are used in refinement. The large reported density is a result of using EADP restraints to model the positional disorder. But the overall quality of the data was poor due to the highly sensitive and unstable nature of the compound that rendered the crystal quality low.

Refinement of 3 (second refinement): Building on the first refinement, some minimal attempts were made to get the most out of the structural model. Specifically, seven highly correlated water molecules that were missed by solvent masking using "Use Solvent Mask results" were modeled, and non-hydrogen atoms were anisotropically manipulated. The ligand shows a high degree of disorder. C077~C07S, O46A~O46, C9~C07R, C2~C235, CXG~CXF, C8~CXE, C69A~C69, C07G~C07F, O51A~O51, C7~C082, N5A~N5, C0~C059, C5~C06W, C07X~C07W, C4~C04W, C3~C03X, C64~C1, O60~O60A, and O64~O64A were disordered over two sites with occupancies 0.516:0.484. In addition, limitation commands such as ISOR, SIMU, SADI, DFIX, and RIGU are used in refinement. But the overall quality of the data was poor due to the highly sensitive and unstable nature of the compound that rendered the crystal quality low.
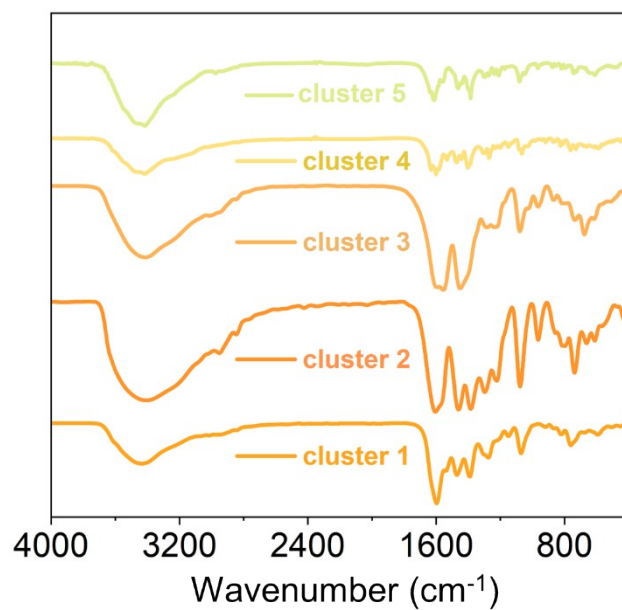
Figure S3. IR spectra of clusters **1**–**5**.
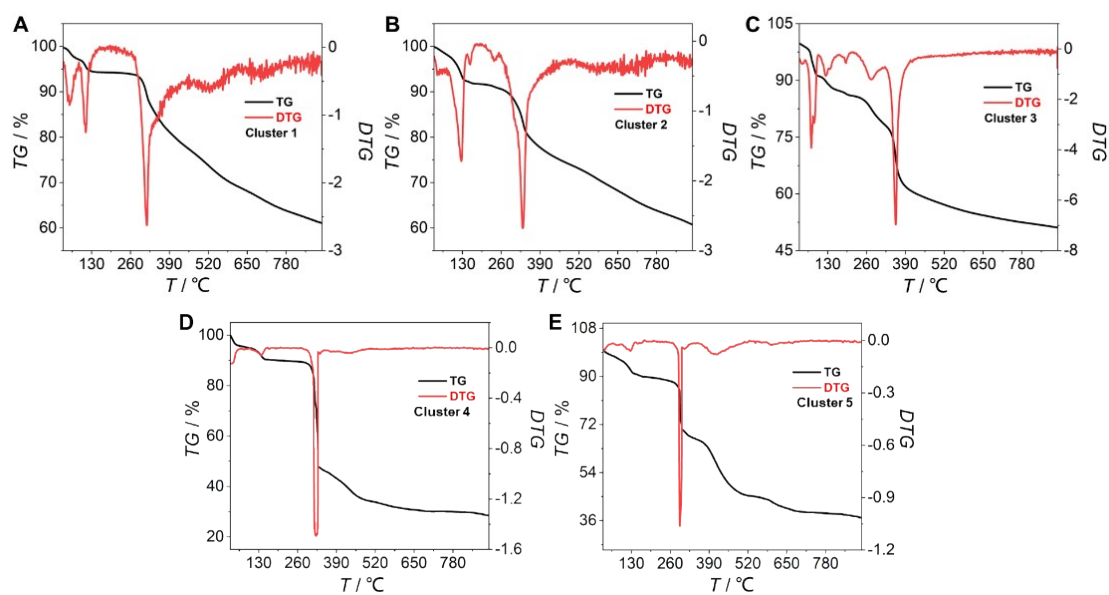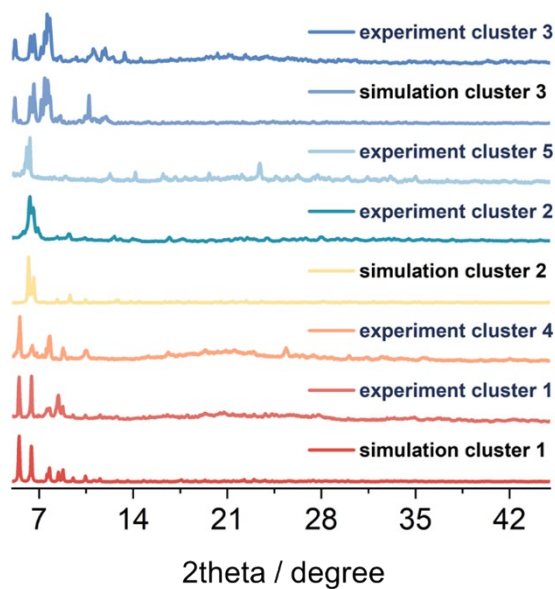
Figure S4. Thermogravimetric curves of clusters **1**–**5**.

Figure S5. Powder X-ray diffraction patterns (PXRD) of clusters **1**–**5**.
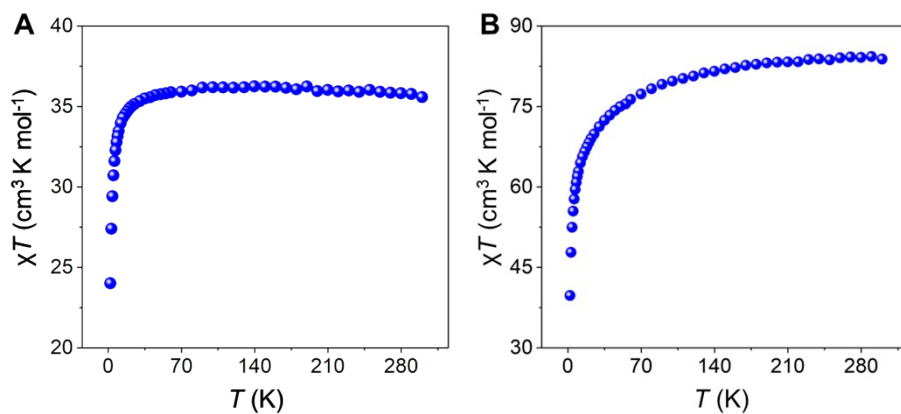
Figure S6. Temperature dependence of $\chi_{m}T$ for clusters **4** and **5** (A and B).
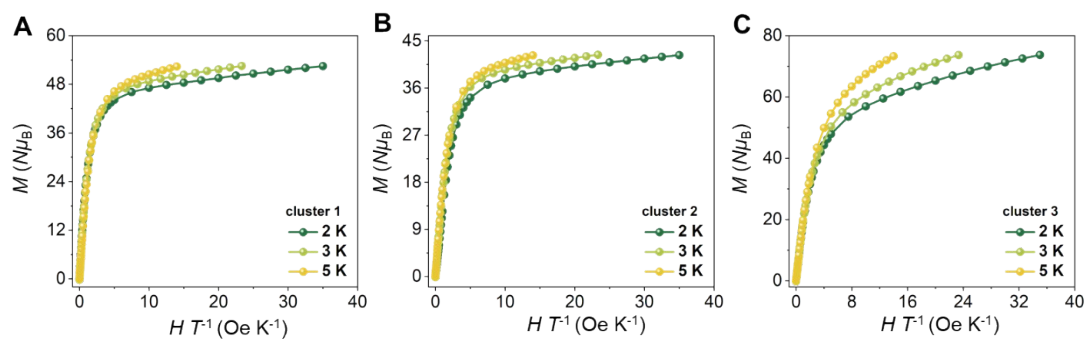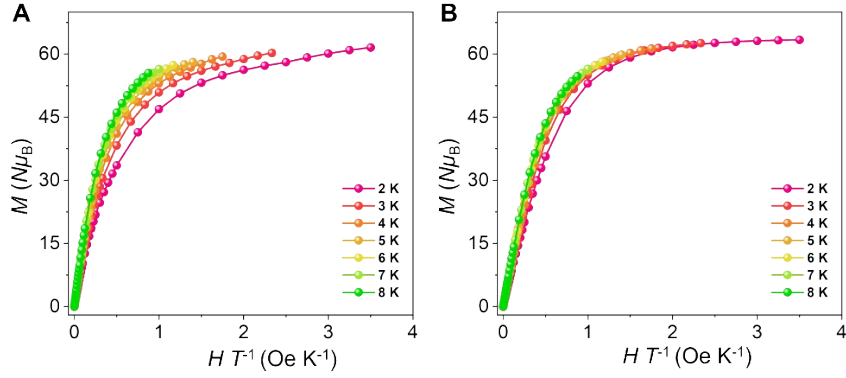
Figure S7. M vs. H/T plots of clusters **1**–**3** (A–C).

Figure S8. *M* vs. *H*/*T* plots of clusters **4** and **5** (A and B).
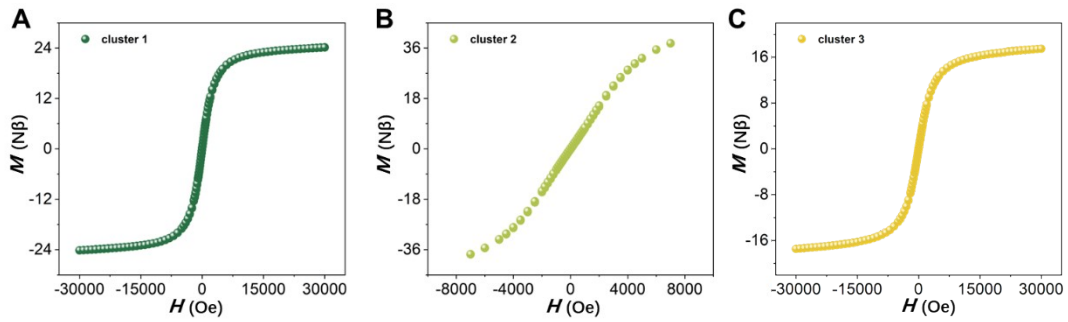
Figure S9. Loop curve graph of clusters **1**–**3** at 2 K.
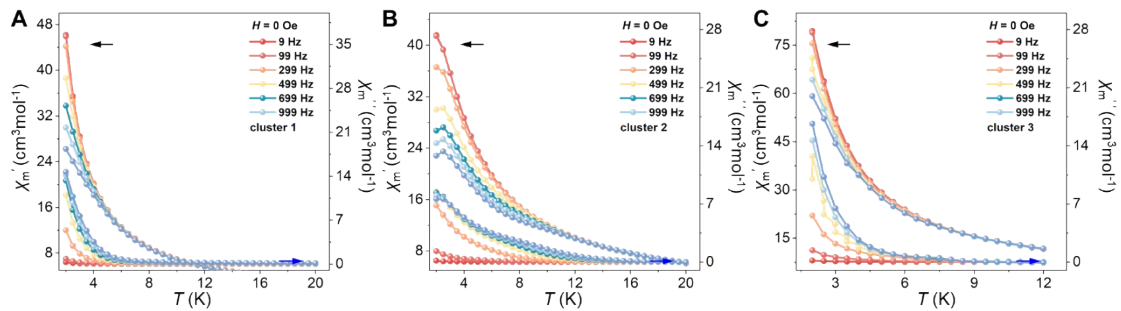
Figure S10. Temperature dependence of the real (χ') and imaginary (χ'') ac susceptibilities at different frequencies in the 0 Oe dc fields for clusters **1**–**3**.
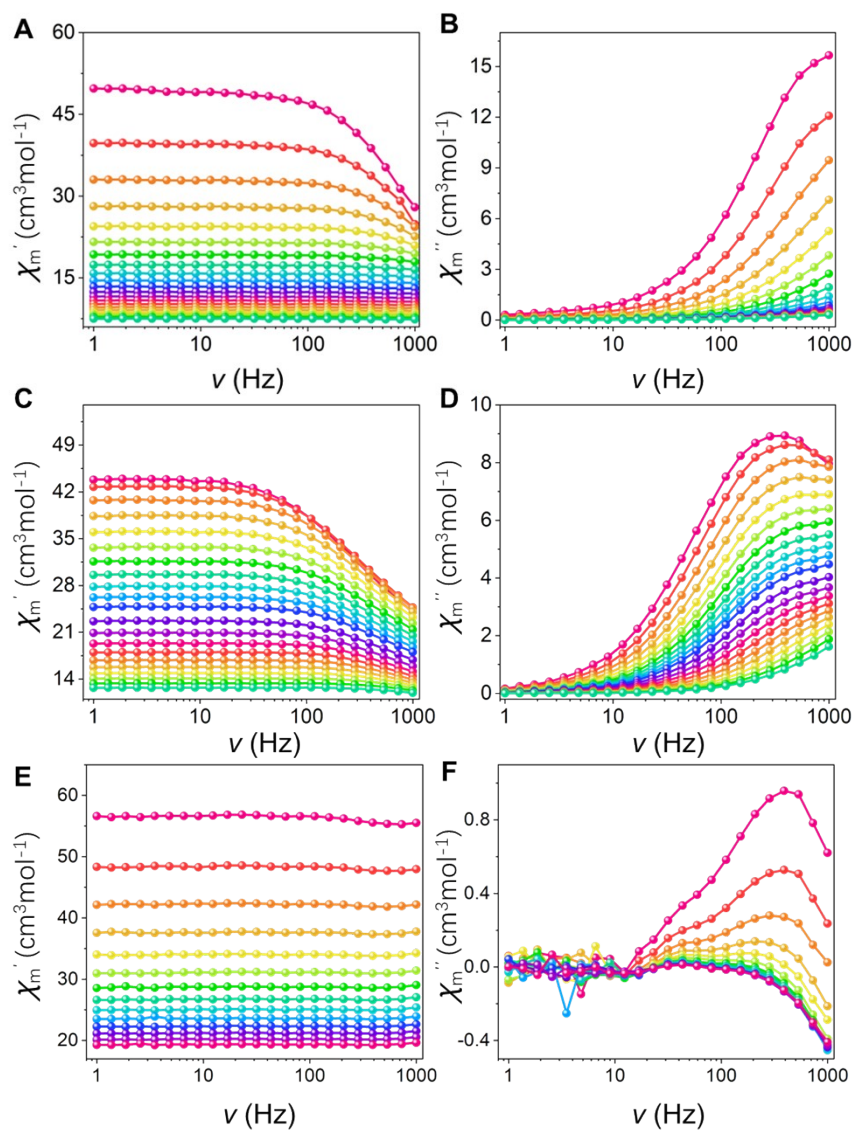
Figure S11. Frequency-dependent χ' and χ'' curves under zero fields for clusters **1**–**3**.
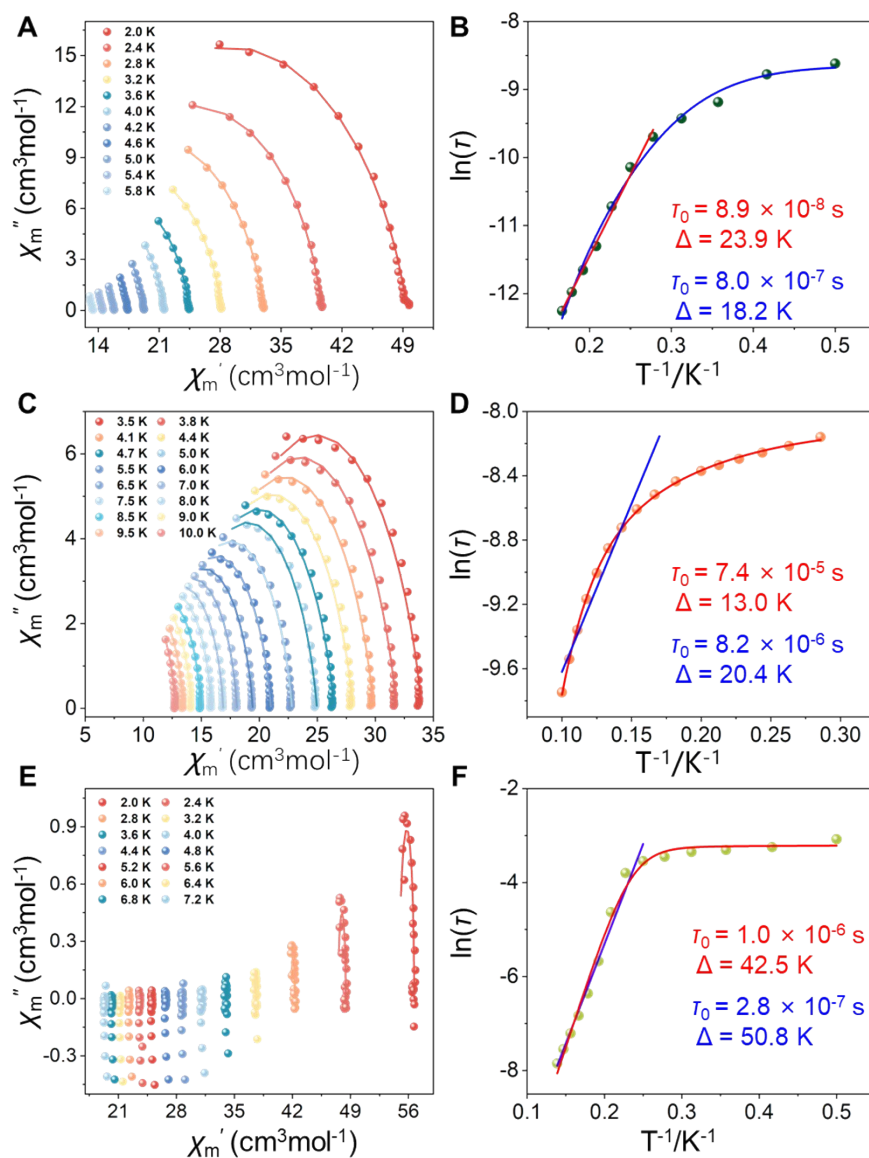
Figure S12. Energy barrier fits under 0 Oe dc field for clusters **1**–**3**.

Table S2. Selected bond lengths (Å) and angles (°) of clusters **1**–**3**.

Bond lengths for cluster 1 (Å)					
Dy1-O3	2.316(3)	Dy2-O6	2.320(3)	Dy4-O15	2.531(3)
Dy1-O37	2.467(3)	Dy2-O1	2.203(3)	Dy4-O14	2.527(3)
Dy1-O8	2.220(3)	Dy3-O15	2.310(3)	Dy4-O18	2.524(3)
Dy1-O16	2.345(3)	Dy3-O11	2.344(3)	Dy4-O2	2.426(3)
Dy1-O7	2.513(3)	Dy3-O16	2.297(3)	Dy4-O19	2.506(3)
Dy1-O26	2.332(3)	Dy3-O12	2.263(3)	Dy4-O7	2.446(3)
Dy1-O10	2.389(3)	Dy3-O28	2.470(4)	Dy5-O23	2.371(3)
Dy1-N1	2.536(4)	Dy3-O26	2.380(3)	Dy5-O19	2.315(3)

Dy2-O2	2.548(3)	Dy3-O27	2.413(3)	Dy5-O24	2.273(3)
Dy2-O20	2.339(3)	Dy3-N4	2.494(4)	Dy5-O20	2.290(3)
Dy2-O25	2.340(3)	Dy4-O26	2.411(3)	Dy5-O25	2.360(3)
Dy2-N2	2.506(4)	Dy4-O25	2.411(3)	Dy5-O33	2.462(3)
Dy2-O22	2.369(3)	Dy4-O30	2.444(3)	Dy5-O34	2.427(3)
Dy2-O36	2.464(3)	Dy4-O31	2.464(3)	Dy5-N6	2.485(4)

Bond angles for cluster 1 (°)

O10-Dy1-N1	124.94(12)	O25-Dy2-O2	63.70(10)	O26-Dy4-O18	68.91(10)
O10-Dy1-O37	71.23(11)	O25-Dy2-N2	133.15(12)	O31-Dy4-O15	72.49(11)
O10-Dy1-O7	140.60(11)	N2-Dy2-O2	70.49(11)	O31-Dy4-O14	71.75(11)
O26-Dy1-O37	72.02(11)	O27-Dy3-N4	133.88(12)	O31-Dy4-O18	112.64(11)
O26-Dy1-O16	74.59(11)	O27-Dy3-O28	52.48(12)	O31-Dy4-O19	77.90(11)
O26-Dy1-O7	63.42(10)	O15-Dy3-O11	143.26(11)	O7-Dy4-O15	71.51(10)
O26-Dy1-O10	87.14(11)	O15-Dy3-O28	75.94(12)	O7-Dy4-O14	71.56(11)
O26-Dy1-N1	133.11(12)	O15-Dy3-O26	70.32(11)	O7-Dy4-O18	104.71(10)
O7-Dy1-N1	71.09(12)	O15-Dy3-O27	89.32(12)	O7-Dy4-O19	140.74(10)
O16-Dy1-O37	132.59(11)	O15-Dy3-N4	71.42(12)	O7-Dy4-O31	139.54(11)
O16-Dy1-O7	72.86(11)	O11-Dy3-O28	117.90(11)	O19-Dy4-O15	147.42(10)
O16-Dy1-O10	74.45(11)	O11-Dy3-O26	75.50(11)	O19-Dy4-O14	130.09(11)
O16-Dy1-N1	82.05(12)	O11-Dy3-O27	76.92(12)	O19-Dy4-O18	51.21(10)
O8-Dy1-O3	84.42(12)	O11-Dy3-N4	140.61(12)	O2-Dy4-O15	139.61(10)
O8-Dy1-O37	83.04(12)	O16-Dy3-O15	105.86(11)	O2-Dy4-O14	104.75(10)
O8-Dy1-O16	120.19(12)	O16-Dy3-O11	76.92(11)	O2-Dy4-O18	71.00(10)
O8-Dy1-O7	138.76(11)	O16-Dy3-O28	153.52(11)	O2-Dy4-O19	72.62(10)
O8-Dy1-O26	153.99(12)	O16-Dy3-O26	74.56(10)	O2-Dy4-O7	69.78(10)
O8-Dy1-O10	77.72(12)	O16-Dy3-O27	151.91(12)	O2-Dy4-O31	136.84(11)
O8-Dy1-N1	72.51(13)	O16-Dy3-N4	74.06(12)	O2-Dy4-O30	140.81(11)
O37-Dy1-O7	118.23(11)	O12-Dy3-O15	142.82(12)	O18-Dy4-O15	131.00(10)
O37-Dy1-N1	145.03(12)	O12-Dy3-O11	72.83(12)	O18-Dy4-O14	175.31(10)
O3-Dy1-O7	71.67(11)	O12-Dy3-O16	88.42(12)	O14-Dy4-O15	51.11(10)
O3-Dy1-O26	94.30(11)	O12-Dy3-O28	76.62(13)	O34-Dy5-O33	52.64(12)
O3-Dy1-O10	140.14(11)	O12-Dy3-O26	146.70(12)	O34-Dy5-N6	134.63(12)
O3-Dy1-N1	81.44(12)	O12-Dy3-O27	93.48(13)	O33-Dy5-N6	82.46(13)
O3-Dy1-O16	144.09(11)	O12-Dy3-N4	80.28(12)	O25-Dy5-O23	76.10(11)

O3-Dy1-O37	71.44(11)	O28-Dy3-N4	81.88(12)	O25-Dy5-O33	127.77(12)
O6-Dy2-O22	140.31(11)	O26-Dy3-O28	128.65(11)	O25-Dy5-O34	87.43(12)
O6-Dy2-O36	72.26(11)	O26-Dy3-O27	89.15(11)	O25-Dy5-N6	121.58(12)
O6-Dy2-O2	70.41(10)	O26-Dy3-N4	120.35(11)	O20-Dy5-O23	76.48(11)
O6-Dy2-O20	143.31(11)	O30-Dy4-O15	76.61(11)	O20-Dy5-O19	106.88(11)
O6-Dy2-O25	92.73(11)	O30-Dy4-O14	112.70(11)	O20-Dy5-O25	75.97(11)
O6-Dy2-N2	80.56(12)	O30-Dy4-O18	71.87(11)	O20-Dy5-O33	153.53(12)
O1-Dy2-O6	81.18(12)	O30-Dy4-O19	74.65(11)	O20-Dy5-O34	151.48(11)
O1-Dy2-O22	78.69(12)	O30-Dy4-O7	132.72(11)	O20-Dy5-N6	73.72(12)
O1-Dy2-O36	81.38(11)	O30-Dy4-O31	52.24(12)	O24-Dy5-O23	71.61(12)
O1-Dy2-O2	136.47(11)	O25-Dy4-O15	117.12(11)	O24-Dy5-O19	143.22(11)
O1-Dy2-O20	124.29(12)	O25-Dy4-O14	68.18(10)	O24-Dy5-O20	88.29(12)
O1-Dy2-O25	152.18(12)	O25-Dy4-O18	110.86(11)	O24-Dy5-O25	146.60(11)
O1-Dy2-N2	72.88(13)	O25-Dy4-O2	64.62(11)	O24-Dy5-O33	76.24(12)
O22-Dy2-O36	71.15(11)	O25-Dy4-O19	66.22(10)	O24-Dy5-O34	93.45(13)
O22-Dy2-O2	142.72(10)	O25-Dy4-O7	106.11(10)	O24-Dy5-N6	80.20(13)
O22-Dy2-N2	124.39(12)	O25-Dy4-O31	74.98(11)	O19-Dy5-O23	143.79(11)
O36-Dy2-O2	118.17(10)	O25-Dy4-O30	119.34(11)	O19-Dy5-O25	70.16(11)
O36-Dy2-N2	145.00(12)	O26-Dy4-O7	63.37(10)	O19-Dy5-O33	75.97(12)
O20-Dy2-O22	75.23(11)	O26-Dy4-O31	116.40(11)	O19-Dy5-O34	88.46(12)
O20-Dy2-O36	131.87(11)	O26-Dy4-O25	168.15(10)	O19-Dy5-N6	72.70(12)
O20-Dy2-O2	73.25(10)	O26-Dy4-O30	72.23(11)	O23-Dy5-O34	77.10(11)
O20-Dy2-O25	75.43(11)	O26-Dy4-O2	105.12(10)	O23-Dy5-N6	139.18(12)
O20-Dy2-N2	82.87(12)	O26-Dy4-O19	117.79(10)	O23-Dy5-O33	117.27(12)
O25-Dy2-O22	89.53(11)	O26-Dy4-O15	66.22(10)		
O25-Dy2-O36	70.94(11)	O26-Dy4-O14	111.02(10)		

Bond lengths for cluster 2 (Å)

Dy1-O7	2.646(3)	Dy2-O22	2.400(3)	Dy3^i-O12	2.531(3)
Dy1-O16	2.295(3)	Dy2-O23	2.526(3)	Dy3^i-O11	2.490(3)
Dy1-O6	2.332(3)	Dy2-O24	2.505(3)	Dy4^i-O17	2.405(3)
Dy1-O14	2.486(3)	Dy2-O5	2.532(3)	Dy3-O19	2.494(3)
Dy1-O9^i	2.339(3)	Dy2-N3	2.514(4)	Dy3-O18	2.434(3)
Dy1-O15	2.261(3)	Dy3-O16	2.277(3)	Dy4-O6	2.325(3)
Dy1-O13	2.387(3)	Dy3-O12^i	2.531(3)	Dy4-O4	2.314(3)

Dy1-O22	2.323(3)	Dy3-O8[i]	2.893(3)	Dy4-O8	2.310(3)
Dy1[i]-O9	2.339(3)	Dy3-O17	2.302(3)	Dy4-O17[i]	2.405(3)
Dy2[i]-O17	2.367(3)	Dy3-O15	2.259(3)	Dy4-O3	2.271(3)
Dy2-O4	2.353(3)	Dy3-O11[i]	2.490(3)	Dy4-O22	2.360(3)
Dy2-O12	2.299(3)	Dy3-O20	2.489(3)	Dy4-N1	2.526(4)
Dy2-O17[i]	2.367(3)	Dy3[i]-O8	2.893(3)	Dy4-N2	2.537(4)
Dy2-O13	2.343(3)				

Bond angles for cluster 2 (°)

O16-Dy1-O7	121.86(10)	O17[i]-Dy2-N3	151.38(11)	O11[i]-Dy3-O8[i]	146.96(9)
O16-Dy1-O6	82.85(10)	O13-Dy2-O4	74.40(10)	O11[i]-Dy3-O19	68.12(10)
O16-Dy1-O14	150.79(10)	O13-Dy2-O17[i]	125.35(10)	O20-Dy3-O12[i]	75.43(10)
O16-Dy1-O9[i]	87.80(10)	O17[i]-Dy2-O24	67.96(10)	O20-Dy3-O8[i]	132.10(9)
O16-Dy1-O13	148.18(10)	O17[i]-Dy2-O5	125.11(10)	O20-Dy3-O11[i]	79.95(10)
O16-Dy1-O22	82.04(10)	O13-Dy2-O22	66.00(10)	O20-Dy3-O19	51.42(10)
O6-Dy1-O7	62.56(9)	O13-Dy2-O23	129.48(10)	O12[i]-Dy3-O8[i]	111.83(9)
O6-Dy1-O14	123.38(10)	O13-Dy2-O24	140.44(10)	O19-Dy3-O8[i]	134.51(10)
O6-Dy1-O9[i]	145.98(10)	O13-Dy2-O5	69.49(10)	O18-Dy3-O12[i]	139.26(10)
O6-Dy1-O13	90.23(10)	O13-Dy2-N3	68.63(11)	O18-Dy3-O8[i]	67.18(10)
O14-Dy1-O7	69.06(10)	O22-Dy2-O23	156.87(10)	O18-Dy3-O11[i]	139.76(10)
O9[i]-Dy1-O7	145.57(10)	O22-Dy2-O24	131.82(10)	O18-Dy3-O20	77.58(11)
O9[i]-Dy1-O14	76.58(10)	O22-Dy2-O5	126.07(10)	O18-Dy3-O19	71.75(11)
O9[i]-Dy1-O13	80.74(10)	O22-Dy2-N3	107.51(10)	O19-Dy3-O12[i]	111.85(10)
O15-Dy1-O7	85.61(10)	O23-Dy2-O5	76.95(10)	O6-Dy4-O17[i]	131.46(10)
O15-Dy1-O16	71.08(10)	O24-Dy2-O23	50.65(10)	O6-Dy4-O22	68.80(10)
O15-Dy1-O6	118.43(11)	O24-Dy2-O5	73.42(10)	O6-Dy4-N1	70.95(11)
O15-Dy1-O14	83.87(10)	O24-Dy2-N3	119.41(11)	O6-Dy4-N2	83.40(11)
O15-Dy1-O9[i]	88.72(11)	N3-Dy2-O23	70.34(11)	O4-Dy4-O6	84.15(10)
O15-Dy1-O13	137.51(10)	N3-Dy2-O5	82.14(11)	O4-Dy4-O17[i]	69.81(10)
O15-Dy1-O22	150.05(10)	O16-Dy3-O12[i]	72.83(9)	O4-Dy4-O22	76.26(10)
O13-Dy1-O7	80.79(10)	O16-Dy3-O8[i]	69.30(9)	O4-Dy4-N1	141.42(11)
O13-Dy1-O14	53.67(10)	O16-Dy3-O17	103.90(10)	O4-Dy4-N2	72.26(11)
O22-Dy1-O7	120.70(9)	O16-Dy3-O11[i]	78.41(10)	O8-Dy4-O6	110.03(10)
O22-Dy1-O6	69.31(10)	O16-Dy3-O20	147.17(10)	O8-Dy4-O4	142.69(10)
O22-Dy1-O14	117.26(10)	O16-Dy3-O19	137.03(10)	O8-Dy4-O17[i]	75.49(10)

O22-Dy1-O9[i]	77.05(10)	O16-Dy3-O18	133.65(11)	O8-Dy4-O22	77.34(10)
O22-Dy1-O13	66.53(10)	O17-Dy3-O12[i]	70.84(9)	O8-Dy4-N1	75.10(11)
O4-Dy2-O17[i]	69.81(10)	O17-Dy3-O8[i]	66.40(9)	O8-Dy4-N2	141.51(11)
O4-Dy2-O22	74.76(10)	O17-Dy3-O11[i]	130.74(10)	O17[i]-Dy4-N1	148.24(11)
O4-Dy2-O23	123.19(10)	O17-Dy3-O20	72.80(10)	O17[i]-Dy4-N2	123.09(11)
O4-Dy2-O24	78.02(10)	O17-Dy3-O19	118.18(10)	O3-Dy4-O6	150.90(11)
O4-Dy2-O5	65.12(10)	O17-Dy3-O18	72.36(11)	O3-Dy4-O4	103.65(11)
O12-Dy2-O4	141.50(10)	O15-Dy3-O16	71.43(10)	O3-Dy4-O8	80.85(11)
O12-Dy2-O17[i]	73.95(10)	O15-Dy3-O12[i]	136.19(10)	O3-Dy4-O17[i]	76.82(10)
O12-Dy2-O13	119.04(10)	O15-Dy3-O8[i]	77.77(10)	O3-Dy4-O22	140.14(11)
O12-Dy2-O22	78.91(10)	O15-Dy3-O17	142.59(11)	O3-Dy4-N1	86.90(11)
O12-Dy2-O23	78.17(10)	O15-Dy3-O11[i]	85.66(10)	O3-Dy4-N2	72.80(12)
O12-Dy2-O24	100.19(10)	O15-Dy3-O20	130.95(10)	O22-Dy4-O17[i]	65.65(10)
O12-Dy2-O5	151.96(10)	O15-Dy3-O19	79.67(10)	O22-Dy4-N1	118.44(10)
O12-Dy2-N3	77.46(11)	O15-Dy3-O18	84.45(11)	O22-Dy4-N2	139.69(11)
O17[i]-Dy2-O22	65.61(9)	O11[i]-Dy3-O12[i]	62.90(9)	N1-Dy4-N2	75.92(11)
O17[i]-Dy2-O23	104.69(10)				

Bond lengths for cluster 3 (Å)

Dy1-O4	2.721(15)	Dy5-O65	2.473(16)	Dy10-O34	2.518(16)
Dy1-O3	2.288(16)	Dy6-O62	2.398(15)	Dy10-O28	2.240(16)
Dy1-O5	2.395(14)	Dy6-O54	2.361(17)	Dy10-O36	2.446(16)
Dy1-O84	2.367(15)	Dy6-O63	2.353(18)	Dy10-O37	2.488(17)
Dy1-O86	2.376(14)	Dy6-O61	2.461(15)	Dy10-O29	2.441(15)
Dy1-O85	2.441(15)	Dy6-O59	2.530(17)	Dy10-O38	2.416(17)
Dy1-O1	2.263(14)	Dy6-O58	2.451(16)	Dy10-O32	2.479(17)
Dy1-O87	2.377(16)	Dy6-O60	2.51(4)	Dy11-O31	2.419(17)
Dy1-N1	2.596(17)	Dy6-O57	2.330(16)	Dy11-O30	2.701(15)
Dy2-O81	2.438(14)	Dy6-O55A	2.444(18)	Dy11-O24	2.361(16)
Dy2-O00Q	2.514(15)	Dy6-O60A	2.46(4)	Dy11-O25	2.452(15)
Dy2-O84	2.472(16)	Dy7-O49	2.328(15)	Dy11-O26	2.416(16)
Dy2-O80	2.306(17)	Dy7-O50	2.482(18)	Dy11-O27	2.353(17)
Dy2-O82	2.521(15)	Dy7-O54	2.791(17)	Dy11-O29	2.278(14)
Dy2-O85	2.386(17)	Dy7-O52	2.396(16)	Dy11-O22	2.337(15)
Dy2-O87	2.329(14)	Dy7-O53	2.388(14)	Dy11-N3	2.58(2)

Dy2-O83	2.371(14)	Dy7-O56	2.292(16)	Dy12-O16	2.419(15)
Dy2-O77	2.364(14)	Dy7-O51	2.18(3)	Dy12-O17	2.365(17)
Dy3-O72	2.353(15)	Dy7-N5	2.52(3)	Dy12-O24	2.418(14)
Dy3-O81	2.300(14)	Dy7-O55A	2.296(18)	Dy12-O20	2.442(16)
Dy3-O79	2.361(17)	Dy7-N5A	2.57(3)	Dy12-O25	2.391(15)
Dy3-O76	2.369(17)	Dy7-O51A	2.39(3)	Dy12-O23	2.439(15)
Dy3-O73	2.355(17)	Dy8-O45	2.489(16)	Dy12-O21	2.558(17)
Dy3-O023	2.467(14)	Dy8-O51	2.44(3)	Dy12-O15	2.299(14)
Dy3-O78	2.434(16)	Dy8-O48	2.366(17)	Dy12-O22	2.356(16)
Dy3-O77	2.820(15)	Dy8-O46	2.53(3)	Dy13-O9	2.285(14)
Dy3-N7	2.579(19)	Dy8-O51A	2.26(3)	Dy13-O12	2.500(16)
Dy4-O72	2.459(15)	Dy8-O46A	2.51(3)	Dy13-O16	2.290(16)
Dy4-O69	2.419(16)	Dy8-O49	2.505(18)	Dy13-O17	2.795(14)
Dy4-O71	2.412(16)	Dy8-O50	2.394(16)	Dy13-O13	2.347(15)
Dy4-O73	2.344(15)	Dy8-O41	2.359(14)	Dy13-O11	2.376(16)
Dy4-O70	2.503(16)	Dy8-O43	2.291(17)	Dy13-O18	2.411(14)
Dy4-O023	2.416(18)	Dy8-O44	2.482(18)	Dy13-O14	2.331(15)
Dy4-O66	2.355(17)	Dy9-O42	2.290(15)	Dy13-N2	2.550(19)
Dy4-O68	2.270(16)	Dy9-O38	2.469(15)	Dy14-O4	2.368(15)
Dy4-O74	2.529(18)	Dy9-O40	2.453(17)	Dy14-O3	2.427(15)
Dy5-O02N	2.406(17)	Dy9-N4	2.588(19)	Dy14-O12	2.391(14)
Dy5-O67	2.284(18)	Dy9-O41	2.750(18)	Dy14-O10	2.449(14)
Dy5-N6	2.60(2)	Dy9-O37	2.373(15)	Dy14-O2	2.296(15)
Dy5-O63	2.298(14)	Dy9-O44	2.253(16)	Dy14-O8	2.520(14)
Dy5-O66	2.681(14)	Dy9-O35	2.327(18)	Dy14-O6	2.487(14)
Dy5-O61	2.401(16)	Dy9-O39	2.443(16)	Dy14-O11	2.458(14)
Dy5-O62	2.472(18)	Dy10-O35	2.344(14)	Dy14-O9	2.377(17)
Dy5-O69	2.310(16)	Dy10-O30	2.353(15)		

Bond angles for cluster 3 (°)

O3-Dy1-O4	64.5(5)	O62-Dy6-O61	68.2(5)	O40-Dy9-N4	136.4(6)
O3-Dy1-O5	82.4(5)	O62-Dy6-O59	132.2(6)	N4-Dy9-O41	130.5(6)
O3-Dy1-O84	138.6(5)	O62-Dy6-O58	119.5(5)	O35-Dy10-O30	145.7(6)
O3-Dy1-O86	90.1(5)	O62-Dy6-O60	81.0(9)	O35-Dy10-O34	63.5(5)
O3-Dy1-O85	139.7(5)	O62-Dy6-O55A	73.0(5)	O35-Dy10-O36	95.0(5)
O3-Dy1-O87	140.3(5)	O62-Dy6-O60A	87.2(8)	O35-Dy10-O37	70.8(5)

O3-Dy1-N1	70.0(6)	O54-Dy6-O62	82.8(5)	O35-Dy10-O29	117.6(5)
O5-Dy1-O4	49.1(4)	O54-Dy6-O61	82.9(6)	O35-Dy10-O38	68.8(5)
O5-Dy1-O85	73.6(5)	O54-Dy6-O59	144.2(5)	O35-Dy10-O32	75.7(5)
O5-Dy1-N1	140.9(6)	O54-Dy6-O58	85.7(6)	O30-Dy10-O34	145.2(5)
O84-Dy1-O4	74.7(5)	O54-Dy6-O60	122.7(11)	O30-Dy10-O36	83.6(5)
O84-Dy1-O5	75.9(5)	O54-Dy6-O55A	68.2(5)	O30-Dy10-O37	81.8(5)
O84-Dy1-O86	117.7(5)	O54-Dy6-O60A	117.1(10)	O30-Dy10-O29	66.5(5)
O84-Dy1-O85	65.5(5)	O63-Dy6-O62	68.4(6)	O30-Dy10-O38	82.0(5)
O84-Dy1-O87	71.7(5)	O63-Dy6-O54	145.7(5)	O30-Dy10-O32	119.4(5)
O84-Dy1-N1	142.5(6)	O63-Dy6-O61	69.7(5)	O28-Dy10-O35	134.5(6)
O86-Dy1-O4	120.6(5)	O63-Dy6-O59	64.5(5)	O28-Dy10-O30	79.4(6)
O86-Dy1-O5	76.4(5)	O63-Dy6-O58	92.4(6)	O28-Dy10-O34	72.5(5)
O86-Dy1-O85	53.4(5)	O63-Dy6-O60	72.0(10)	O28-Dy10-O36	82.4(6)
O86-Dy1-O87	94.3(5)	O63-Dy6-O55A	117.3(5)	O28-Dy10-O37	132.7(6)
O86-Dy1-N1	76.5(5)	O63-Dy6-O60A	80.8(9)	O28-Dy10-O29	78.4(6)
O85-Dy1-O4	116.2(4)	O61-Dy6-O59	101.8(6)	O28-Dy10-O38	149.6(5)
O85-Dy1-N1	110.6(5)	O61-Dy6-O60	137.4(9)	O28-Dy10-O32	85.0(6)
O1-Dy1-O4	77.7(5)	O61-Dy6-O60A	146.7(8)	O36-Dy10-O34	72.9(5)
O1-Dy1-O3	85.5(5)	O58-Dy6-O61	51.4(5)	O36-Dy10-O37	52.5(5)
O1-Dy1-O5	125.3(5)	O58-Dy6-O59	71.0(5)	O36-Dy10-O32	151.0(5)
O1-Dy1-O84	79.2(5)	O58-Dy6-O60	148.4(11)	O37-Dy10-O34	102.4(5)
O1-Dy1-O86	156.8(5)	O58-Dy6-O60A	148.0(9)	O29-Dy10-O34	125.0(6)
O1-Dy1-O85	134.8(6)	O60-Dy6-O59	77.4(10)	O29-Dy10-O36	146.9(5)
O1-Dy1-O87	75.3(5)	O57-Dy6-O62	149.0(6)	O29-Dy10-O37	131.0(6)
O1-Dy1-N1	80.6(5)	O57-Dy6-O54	75.9(5)	O29-Dy10-O32	53.0(5)
O87-Dy1-O4	140.0(5)	O57-Dy6-O63	137.6(6)	O38-Dy10-O34	131.8(5)
O87-Dy1-O5	137.0(5)	O57-Dy6-O61	129.6(5)	O38-Dy10-O36	119.2(6)
O87-Dy1-O85	67.6(5)	O57-Dy6-O59	74.0(6)	O38-Dy10-O37	67.0(5)
O87-Dy1-N1	72.7(6)	O57-Dy6-O58	81.5(5)	O38-Dy10-O29	72.1(5)
N1-Dy1-O4	130.6(5)	O57-Dy6-O60	91.7(9)	O38-Dy10-O32	83.5(6)
O81-Dy2-O00Q	126.5(5)	O57-Dy6-O55A	78.3(6)	O32-Dy10-O34	78.5(5)
O81-Dy2-O84	129.9(5)	O57-Dy6-O60A	82.9(8)	O32-Dy10-O37	141.4(5)
O81-Dy2-O82	51.9(5)	O55A-Dy6-O61	133.9(5)	O31-Dy11-O30	49.3(5)
O00Q-Dy2-O82	80.5(5)	O55A-Dy6-O59	122.9(5)	O31-Dy11-O25	75.4(5)

O84-Dy2-O00Q	101.6(5)	O55A-Dy6-O58	150.1(6)	O31-Dy11-N3	139.3(6)
O84-Dy2-O82	140.3(5)	O55A-Dy6-O60	54.5(11)	O24-Dy11-O31	78.2(5)
O80-Dy2-O81	81.0(5)	O55A-Dy6-O60A	49.6(10)	O24-Dy11-O30	77.5(5)
O80-Dy2-O00Q	72.8(5)	O60A-Dy6-O59	77.8(10)	O24-Dy11-O25	66.6(5)
O80-Dy2-O84	131.8(5)	O49-Dy7-O50	66.0(6)	O24-Dy11-O26	118.4(5)
O80-Dy2-O82	87.1(5)	O49-Dy7-O54	74.6(5)	O24-Dy11-N3	141.5(6)
O80-Dy2-O85	150.9(5)	O49-Dy7-O52	117.1(6)	O25-Dy11-O30	119.0(5)
O80-Dy2-O87	134.7(5)	O49-Dy7-O53	76.3(5)	O25-Dy11-N3	108.2(6)
O80-Dy2-O83	81.5(5)	O49-Dy7-N5	144.7(7)	O26-Dy11-O31	76.5(6)
O80-Dy2-O77	78.4(6)	O49-Dy7-N5A	144.1(7)	O26-Dy11-O30	120.3(5)
O85-Dy2-O81	71.9(5)	O49-Dy7-O51A	74.2(8)	O26-Dy11-O25	53.0(5)
O85-Dy2-O00Q	132.5(5)	O50-Dy7-O54	118.9(5)	O26-Dy11-N3	74.9(6)
O85-Dy2-O84	64.8(5)	O50-Dy7-N5	113.9(11)	O27-Dy11-O31	125.0(5)
O85-Dy2-O82	84.4(5)	O50-Dy7-N5A	105.7(10)	O27-Dy11-O30	76.7(5)
O87-Dy2-O81	116.1(5)	O52-Dy7-O50	52.7(5)	O27-Dy11-O24	80.8(6)
O87-Dy2-O00Q	63.4(5)	O52-Dy7-O54	122.1(5)	O27-Dy11-O25	137.5(5)
O87-Dy2-O84	70.7(5)	O52-Dy7-N5	79.5(9)	O27-Dy11-O26	155.4(6)
O87-Dy2-O82	75.4(5)	O52-Dy7-N5A	72.4(9)	O27-Dy11-N3	80.6(6)
O87-Dy2-O85	69.3(5)	O53-Dy7-O50	75.6(6)	O29-Dy11-O31	81.0(6)
O87-Dy2-O83	93.0(5)	O53-Dy7-O54	50.2(5)	O29-Dy11-O30	63.1(5)
O87-Dy2-O77	146.3(6)	O53-Dy7-O52	76.4(5)	O29-Dy11-O24	140.1(5)
O83-Dy2-O81	150.6(5)	O53-Dy7-N5	139.0(7)	O29-Dy11-O25	138.6(6)
O83-Dy2-O00Q	69.3(5)	O53-Dy7-N5A	137.7(7)	O29-Dy11-O26	88.7(5)
O83-Dy2-O84	53.5(5)	O53-Dy7-O51A	137.3(8)	O29-Dy11-O27	83.9(5)
O83-Dy2-O82	149.7(5)	O56-Dy7-O49	78.4(5)	O29-Dy11-O22	139.5(6)
O83-Dy2-O85	118.1(5)	O56-Dy7-O50	134.1(6)	O29-Dy11-N3	70.1(6)
O77-Dy2-O81	68.2(5)	O56-Dy7-O54	75.1(5)	O22-Dy11-O31	138.8(5)
O77-Dy2-O00Q	143.8(5)	O56-Dy7-O52	158.3(5)	O22-Dy11-O30	141.9(5)
O77-Dy2-O84	81.5(5)	O56-Dy7-O53	123.9(6)	O22-Dy11-O24	71.4(6)
O77-Dy2-O82	119.9(5)	O56-Dy7-N5	79.5(9)	O22-Dy11-O25	67.4(5)
O77-Dy2-O85	81.9(5)	O56-Dy7-O55A	84.3(6)	O22-Dy11-O26	94.0(5)
O77-Dy2-O83	85.2(5)	O56-Dy7-N5A	86.2(9)	O22-Dy11-O27	77.1(5)
O72-Dy3-O79	77.6(5)	O56-Dy7-O51A	78.9(9)	O22-Dy11-N3	71.7(6)
O72-Dy3-O76	79.5(6)	O51-Dy7-O49	73.5(9)	N3-Dy11-O30	129.6(5)

O72-Dy3-O73	73.8(5)	O51-Dy7-O50	71.4(9)	O16-Dy12-O20	53.4(6)
O72-Dy3-O023	66.6(5)	O51-Dy7-O54	137.3(10)	O16-Dy12-O23	150.1(5)
O72-Dy3-O78	117.8(5)	O51-Dy7-O52	97.5(11)	O16-Dy12-O21	123.1(5)
O72-Dy3-O77	78.7(5)	O51-Dy7-O53	142.0(9)	O17-Dy12-O16	68.1(5)
O72-Dy3-N7	143.9(6)	O51-Dy7-O56	71.3(11)	O17-Dy12-O24	82.4(5)
O81-Dy3-O72	140.0(5)	O51-Dy7-N5	73.5(11)	O17-Dy12-O20	121.4(5)
O81-Dy3-O79	83.4(5)	O51-Dy7-O55A	136.2(8)	O17-Dy12-O25	82.6(5)
O81-Dy3-O76	82.2(5)	N5-Dy7-O54	125.0(11)	O17-Dy12-O23	86.1(5)
O81-Dy3-O73	134.5(6)	O55A-Dy7-O49	137.2(6)	O17-Dy12-O21	145.5(5)
O81-Dy3-O023	141.8(6)	O55A-Dy7-O50	141.6(5)	O24-Dy12-O16	132.5(5)
O81-Dy3-O78	90.6(5)	O55A-Dy7-O54	63.1(5)	O24-Dy12-O20	139.8(5)
O81-Dy3-O77	62.5(5)	O55A-Dy7-O52	92.2(6)	O24-Dy12-O23	53.2(5)
O81-Dy3-N7	68.8(6)	O55A-Dy7-O53	81.8(5)	O24-Dy12-O21	102.4(5)
O79-Dy3-O76	123.2(5)	O55A-Dy7-N5	66.5(10)	O20-Dy12-O21	76.5(5)
O79-Dy3-O023	134.7(5)	O55A-Dy7-N5A	71.8(9)	O25-Dy12-O16	73.1(5)
O79-Dy3-O78	159.8(5)	O55A-Dy7-O51A	139.9(7)	O25-Dy12-O24	66.7(5)
O79-Dy3-O77	75.7(5)	N5A-Dy7-O54	132.3(10)	O25-Dy12-O20	83.7(5)
O79-Dy3-N7	88.2(6)	O51A-Dy7-O50	64.5(8)	O25-Dy12-O23	119.8(5)
O76-Dy3-O023	77.4(5)	O51A-Dy7-O54	142.6(9)	O25-Dy12-O21	131.0(5)
O76-Dy3-O78	74.6(5)	O51A-Dy7-O52	90.5(9)	O23-Dy12-O20	147.4(6)
O76-Dy3-O77	49.1(5)	O51A-Dy7-N5A	71.0(10)	O23-Dy12-O21	71.0(5)
O76-Dy3-N7	134.6(6)	O49-Dy8-O46	92.4(10)	O15-Dy12-O16	78.2(5)
O73-Dy3-O79	75.9(6)	O49-Dy8-O46A	109.8(10)	O15-Dy12-O17	79.0(5)
O73-Dy3-O76	142.7(5)	O50-Dy8-O49	64.7(5)	O15-Dy12-O24	132.8(5)
O73-Dy3-O023	68.3(6)	O50-Dy8-O44	73.0(6)	O15-Dy12-O20	86.0(5)
O73-Dy3-O78	95.3(5)	O50-Dy8-O45	84.1(5)	O15-Dy12-O25	150.1(5)
O73-Dy3-O77	143.9(5)	O50-Dy8-O51	68.8(7)	O15-Dy12-O23	82.4(5)
O73-Dy3-N7	70.5(6)	O50-Dy8-O46	131.8(7)	O15-Dy12-O21	72.7(5)
O023-Dy3-O77	120.6(5)	O50-Dy8-O46A	133.4(7)	O15-Dy12-O22	134.9(6)
O023-Dy3-N7	104.5(5)	O41-Dy8-O49	81.7(5)	O22-Dy12-O16	116.7(5)
O78-Dy3-O023	53.1(5)	O41-Dy8-O50	81.1(5)	O22-Dy12-O17	145.7(5)
O78-Dy3-O77	118.4(5)	O41-Dy8-O44	67.5(5)	O22-Dy12-O24	70.1(5)
O78-Dy3-N7	71.7(6)	O41-Dy8-O45	119.9(6)	O22-Dy12-O20	74.0(5)
N7-Dy3-O77	129.9(5)	O41-Dy8-O51	142.8(8)	O22-Dy12-O25	68.1(6)

O72-Dy4-O70	144.9(5)	O41-Dy8-O48	85.0(5)	O22-Dy12-O23	93.0(5)
O72-Dy4-O74	100.0(5)	O41-Dy8-O46	139.8(8)	O22-Dy12-O21	63.5(5)
O69-Dy4-O72	132.4(6)	O41-Dy8-O46A	145.6(7)	O9-Dy13-O12	67.8(5)
O69-Dy4-O70	51.1(6)	O43-Dy8-O49	132.7(5)	O9-Dy13-O16	137.8(5)
O69-Dy4-O74	125.5(5)	O43-Dy8-O50	150.2(6)	O9-Dy13-O17	142.7(5)
O71-Dy4-O72	51.7(6)	O43-Dy8-O41	78.9(5)	O9-Dy13-O13	95.7(5)
O71-Dy4-O69	150.0(5)	O43-Dy8-O44	79.1(6)	O9-Dy13-O11	71.9(5)
O71-Dy4-O70	148.3(6)	O43-Dy8-O45	87.0(6)	O9-Dy13-O18	139.5(6)
O71-Dy4-O023	117.0(5)	O43-Dy8-O51	136.9(7)	O9-Dy13-O14	78.1(5)
O71-Dy4-O74	70.9(5)	O43-Dy8-O48	82.7(6)	O9-Dy13-N2	72.3(6)
O73-Dy4-O72	72.1(5)	O43-Dy8-O46	76.3(8)	O12-Dy13-O17	118.8(5)
O73-Dy4-O69	114.0(5)	O43-Dy8-O46A	69.5(8)	O12-Dy13-N2	107.5(5)
O73-Dy4-O71	95.7(5)	O44-Dy8-O49	130.7(5)	O16-Dy13-O12	140.6(5)
O73-Dy4-O70	76.3(5)	O44-Dy8-O45	52.4(5)	O16-Dy13-O17	62.7(5)
O73-Dy4-O023	69.4(6)	O44-Dy8-O46	135.9(10)	O16-Dy13-O13	89.7(6)
O73-Dy4-O66	143.6(6)	O44-Dy8-O46A	117.5(10)	O16-Dy13-O11	140.0(5)
O73-Dy4-O74	63.0(6)	O45-Dy8-O49	139.5(5)	O16-Dy13-O18	82.3(5)
O70-Dy4-O74	78.4(6)	O45-Dy8-O46	90.0(9)	O16-Dy13-O14	81.9(5)
O023-Dy4-O72	65.8(5)	O45-Dy8-O46A	72.8(9)	O16-Dy13-N2	69.1(5)
O023-Dy4-O69	72.7(5)	O51-Dy8-O49	66.2(9)	O13-Dy13-O12	53.4(5)
O023-Dy4-O70	89.2(5)	O51-Dy8-O44	120.3(10)	O13-Dy13-O17	118.0(4)
O023-Dy4-O74	132.4(5)	O51-Dy8-O45	79.2(10)	O13-Dy13-O11	117.5(6)
O66-Dy4-O72	80.4(5)	O51-Dy8-O46	63.1(9)	O13-Dy13-O18	74.9(5)
O66-Dy4-O69	68.8(5)	O48-Dy8-O49	52.7(5)	O13-Dy13-N2	74.5(6)
O66-Dy4-O71	85.1(5)	O48-Dy8-O50	117.2(6)	O11-Dy13-O12	65.8(5)
O66-Dy4-O70	119.6(5)	O48-Dy8-O44	149.4(5)	O11-Dy13-O17	78.2(5)
O66-Dy4-O023	77.9(6)	O48-Dy8-O45	150.7(5)	O11-Dy13-O18	77.8(5)
O66-Dy4-O74	147.4(6)	O48-Dy8-O51	89.7(10)	O11-Dy13-N2	143.1(5)
O68-Dy4-O72	130.2(5)	O48-Dy8-O46	60.9(9)	O18-Dy13-O12	75.5(5)
O68-Dy4-O69	80.5(6)	O48-Dy8-O46A	77.9(9)	O18-Dy13-O17	48.7(5)
O68-Dy4-O71	81.1(5)	O51A-Dy8-O49	73.2(9)	O18-Dy13-N2	137.6(5)
O68-Dy4-O73	135.4(6)	O51A-Dy8-O50	68.0(7)	O14-Dy13-O12	137.5(5)
O68-Dy4-O70	83.6(5)	O51A-Dy8-O41	146.2(8)	O14-Dy13-O17	75.3(5)
O68-Dy4-O023	150.3(6)	O51A-Dy8-O43	134.9(7)	O14-Dy13-O13	158.7(5)

O68-Dy4-O66	80.8(6)	O51A-Dy8-O44	113.3(10)	O14-Dy13-O11	80.3(5)
O68-Dy4-O74	74.2(6)	O51A-Dy8-O45	71.4(10)	O14-Dy13-O18	122.8(5)
O62-Dy5-O65	72.2(5)	O51A-Dy8-O48	97.0(10)	O14-Dy13-N2	84.2(6)
O62-Dy5-O66	117.9(5)	O51A-Dy8-O46A	66.5(9)	N2-Dy13-O17	129.5(5)
O62-Dy5-N6	106.6(6)	O35-Dy9-O39	93.9(6)	O9-Dy14-O3	116.3(5)
O69-Dy5-O62	138.7(6)	O35-Dy9-O41	144.1(5)	O9-Dy14-O12	68.3(5)
O69-Dy5-O65	84.7(5)	O35-Dy9-O37	73.1(6)	O9-Dy14-O10	93.3(5)
O69-Dy5-O66	64.9(5)	O35-Dy9-O38	68.2(5)	O9-Dy14-O6	75.7(5)
O69-Dy5-O61	139.0(5)	O35-Dy9-O40	138.5(5)	O9-Dy14-O11	68.9(5)
O69-Dy5-O02N	89.7(6)	O35-Dy9-N4	72.0(6)	O9-Dy14-O8	65.8(5)
O69-Dy5-N6	69.6(6)	O39-Dy9-O41	117.7(5)	O4-Dy14-O9	145.2(5)
O65-Dy5-O66	51.0(6)	O39-Dy9-O38	52.1(5)	O4-Dy14-O3	68.5(5)
O65-Dy5-N6	138.9(6)	O39-Dy9-O40	73.8(5)	O4-Dy14-O12	82.1(5)
O63-Dy5-O62	68.0(6)	O39-Dy9-N4	73.8(6)	O4-Dy14-O10	84.9(5)
O63-Dy5-O69	139.2(6)	O37-Dy9-O39	118.7(5)	O4-Dy14-O6	121.1(5)
O63-Dy5-O65	135.6(6)	O37-Dy9-O41	76.6(5)	O4-Dy14-O11	82.9(5)
O63-Dy5-O66	140.0(5)	O37-Dy9-O38	68.0(5)	O4-Dy14-O8	143.8(5)
O63-Dy5-O61	71.6(5)	O37-Dy9-O40	78.5(5)	O3-Dy14-O10	150.1(5)
O63-Dy5-O02N	94.3(5)	O37-Dy9-N4	143.7(7)	O3-Dy14-O6	52.9(5)
O63-Dy5-N6	73.0(6)	O44-Dy9-O35	137.1(6)	O3-Dy14-O11	132.3(5)
O61-Dy5-O62	68.0(6)	O44-Dy9-O39	89.9(6)	O3-Dy14-O8	122.3(5)
O61-Dy5-O65	75.8(5)	O44-Dy9-O41	64.2(5)	O12-Dy14-O3	72.4(5)
O61-Dy5-O66	74.9(5)	O44-Dy9-O37	139.4(6)	O12-Dy14-O10	118.6(5)
O61-Dy5-O02N	118.8(6)	O44-Dy9-O42	82.2(6)	O12-Dy14-O6	85.6(5)
O61-Dy5-N6	143.4(5)	O44-Dy9-O38	139.4(6)	O12-Dy14-O11	66.2(5)
O02N-Dy5-O62	52.0(5)	O44-Dy9-O40	83.4(6)	O12-Dy14-O8	133.4(5)
O02N-Dy5-O65	75.7(5)	O44-Dy9-N4	68.2(7)	O10-Dy14-O6	148.0(5)
O02N-Dy5-O66	121.0(5)	O42-Dy9-O35	78.5(6)	O10-Dy14-O11	52.7(5)
O02N-Dy5-N6	72.8(6)	O42-Dy9-O39	158.0(5)	O10-Dy14-O8	72.3(5)
O67-Dy5-O62	138.1(5)	O42-Dy9-O41	77.2(6)	O6-Dy14-O8	75.8(5)
O67-Dy5-O69	83.1(6)	O42-Dy9-O37	79.2(5)	O11-Dy14-O6	140.8(5)
O67-Dy5-O65	125.6(5)	O42-Dy9-O38	138.4(6)	O11-Dy14-O8	103.5(5)
O67-Dy5-O63	77.1(6)	O42-Dy9-O40	125.1(6)	O2-Dy14-O9	135.9(5)
O67-Dy5-O66	76.0(5)	O42-Dy9-N4	84.3(6)	O2-Dy14-O4	78.4(5)

O67-Dy5-O61	79.8(6)	O38-Dy9-O41	117.0(5)	O2-Dy14-O3	79.7(5)
O67-Dy5-O02N	156.4(6)	O38-Dy9-N4	107.3(6)	O2-Dy14-O12	150.4(5)
O67-Dy5-N6	83.6(6)	O40-Dy9-O41	49.1(5)	O2-Dy14-O10	81.7(5)
N6-Dy5-O66	131.7(6)	O40-Dy9-O38	73.4(5)	O2-Dy14-O6	85.7(5)
O2-Dy14-O11	132.0(5)	O2-Dy14-O8	71.0(5)		

Table S3. *SHAPE* analysis of the Dy(III) in cluster **1**.

Label	Symmetry	Shape	Distortion (°) Dy1
OP-8	D_{8h}	Octagon	34.080
HPY-8	C_{7v}	Heptagonal pyramid	22.253
HBPY-8	D_{6h}	Hexagonal bipyramid	15.401
CU-8	O_h	Cube	10.239
SAPR-8	D_{4d}	Square antiprism	2.132
TDD-8	D_{2d}	Triangular dodecahedron	1.592
JGBF-8	D_{2d}	Johnson-Gyrobifastigium (J26)	14.485
JETBPY-8	D_{3h}	Johnson-Elongated triangular bipyramid (J14)	28.082
JBTP-8	C_{2v}	Johnson-Biaugmented trigonal prism (J50)	2.848
BTPR-8	C_{2v}	Biaugmen tedtrigonal prism	2.240
JSD-8	D_{2d}	Snub disphenoid (J84)	3.735
TT-8	T_d	Triakis tetrahedron	10.546
ETBPY-8	D_{3h}	Elongated trigonal bipyramid	24.144

Label	Symmetry	Shape	Distortion (°) Dy2
DP-10	D_{10h}	Decagon	46.126
EPY-10	C_{9v}	Enneagonal pyramid	36.115
OBPY-10	D_{8h}	Octagonal bipyramid	30.540
PPR-10	D_{5h}	Pentagonal prism	26.826
PAPR-10	D_{5d}	Pentagonal antiprism	25.825
JBCCU-10	D_{4h}	Bicapped cube J15	27.505
JBCSAPR-10	D_{4d}	Bicapped square antiprism J17	22.863
JMBIC-10	C_{2v}	Metabidiminished icosahedron J62	22.745
JATDI-10	C_{3v}	Augmented tridiminished icosahedron J64	31.535
JSPC-10	C_{2v}	Sphenocorona J87	20.196
SDD-10	D_2	Staggered Dodecahedron (2:6:2)	21.584
TD-10	C_{2v}	Tetradecahedron (2:6:2)	20.788
HD-10	D_{4h}	Hexadecahedron (2:6:2) or (1:4:4:1)	25.446

Label	Symmetry	Shape	Distortion (°) Dy4
OP-8	D_{8h}	Octagon	29.897
HPY-8	C_{7v}	Heptagonal pyramid	23.267
HBPY-8	D_{6h}	Hexagonal bipyramid	13.706

CU-8	O_h	Cube	8.793
SAPR-8	D_{4d}	Square antiprism	1.458
TDD-8	D_{2d}	Triangular dodecahedron	1.752
JGBF-8	D_{2d}	Johnson-Gyrobifastigium (J26)	12.022
JETBPY-8	D_{3h}	Johnson-Elongated triangular bipyramid (J14)	27.446
JBTP-8	C_{2v}	Johnson-Biaugmented trigonal prism (J50)	1.465
BTPR-8	C_{2v}	Biaugmen tedtrigonal prism	1.057
JSD-8	D_{2d}	Snub disphenoid (J84)	3.829
TT-8	T_d	Triakis tetrahedron	9.608
ETBPY-8	D_{3h}	Elongated trigonal bipyramid	24.050

Table S4. *SHAPE* analysis of the Dy(III) in cluster **2**.

Label	Symmetry	Shape	Distortion (°) Dy1
OP-8	D_{8h}	Octagon	34.465
HPY-8	C_{7v}	Heptagonal pyramid	22.972
HBPY-8	D_{6h}	Hexagonal bipyramid	14.701
CU-8	O_h	Cube	11.772
SAPR-8	D_{4d}	Square antiprism	3.650
TDD-8	D_{2d}	Triangular dodecahedron	2.820
JGBF-8	D_{2d}	Johnson-Gyrobifastigium (J26)	13.742
JETBPY-8	D_{3h}	Johnson-Elongated triangular bipyramid (J14)	27.488
JBTP-8	C_{2v}	Johnson-Biaugmented trigonal prism (J50)	2.968
BTPR-8	C_{2v}	Biaugmen tedtrigonal prism	1.857
JSD-8	D_{2d}	Snub disphenoid (J84)	4.674
TT-8	T_d	Triakis tetrahedron	12.132
ETBPY-8	D_{3h}	Elongated trigonal bipyramid	23.801

Label	Symmetry	Shape	Distortion (°) Dy2
EP-9	D_{9h}	Enneagon	46.536
OPY-9	C_{8v}	Octagonal pyramid	34.740
HBPY-9	D_{7h}	Heptagonal bipyramid	31.628
JTC-9	C_{3v}	Triangular cupola J3	26.164
JCCU-9	C_{4v}	Capped cube (J8)	27.082
CCU-9	C_4	Capped cube	27.029
JCSAPR-9	C_{4v}	Capped sq. antiprism	22.431
CSAPR-9	C_{4v}	Capped square antiprism	22.257
JTCTPR-9	D_{3h}	Tricapped trigonal prism J51	22.557
TCTPR-9	D_{3h}	Tricapped trigonal prism	22.621
JTDIC-9	C_{3v}	Tridiminished icosahedron J63	28.655
HH-9	C_{2v}	Hula-hoop	26.356
MFF-9	C_s	Muffin	22.014

Label	Symmetry	Shape	Distortion (°) Dy3
OP-8	D_{8h}	Octagon	41.248
HPY-8	C_{7v}	Heptagonal pyramid	34.938
HBPY-8	D_{6h}	Hexagonal bipyramid	31.838
CU-8	O_h	Cube	29.750
SAPR-8	D_{4d}	Square antiprism	24.122
TDD-8	D_{2d}	Triangular dodecahedron	22.789
JGBF-8	D_{2d}	Johnson-Gyrobifastigium (J26)	29.793
JETBPY-8	D_{3h}	Johnson-Elongated triangular bipyramid (J14)	39.459
JBTP-8	C_{2v}	Johnson-Biaugmented trigonal prism (J50)	21.273
BTPR-8	C_{2v}	Biaugmen tedtrigonal prism	21.801
JSD-8	D_{2d}	Snub disphenoid (J84)	21.185
TT-8	T_d	Triakis tetrahedron	28.419
ETBPY-8	D_{3h}	Elongated trigonal bipyramid	37.822

Label	Symmetry	Shape	Distortion (°) Dy4
OP-8	D_{8h}	Octagon	46.572
HPY-8	C_{7v}	Heptagonal pyramid	34.998
HBPY-8	D_{6h}	Hexagonal bipyramid	31.262
CU-8	O_h	Cube	29.563
SAPR-8	D_{4d}	Square antiprism	24.153
TDD-8	D_{2d}	Triangular dodecahedron	24.412
JGBF-8	D_{2d}	Johnson-Gyrobifastigium (J26)	32.056
JETBPY-8	D_{3h}	Johnson-Elongated triangular bipyramid (J14)	39.388
JBTP-8	C_{2v}	Johnson-Biaugmented trigonal prism (J50)	23.417
BTPR-8	C_{2v}	Biaugmen tedtrigonal prism	24.874
JSD-8	D_{2d}	Snub disphenoid (J84)	23.475
TT-8	T_d	Triakis tetrahedron	28.260
ETBPY-8	D_{3h}	Elongated trigonal bipyramid	36.324

Table S5. *SHAPE* analysis of the Dy(III) in cluster **3**.

Label	Symmetry	Shape	Distortion (°) Dy1
EP-9	D_{9h}	Enneagon	43.082
OPY-9	C_{8v}	Octagonal pyramid	32.868
HBPY-9	D_{7h}	Heptagonal bipyramid	33.390
JTC-9	C_{3v}	Triangular cupola J3	22.000
JCCU-9	C_{4v}	Capped cube (J8)	27.110
CCU-9	C_4	Capped cube	26.767
JCSAPR-9	C_{4v}	Capped sq. antiprism	22.628
CSAPR-9	C_{4v}	Capped square antiprism	22.144
JTCTPR-9	D_{3h}	Tricapped trigonal prism J51	21.810

Label	Symmetry	Shape	Distortion (°) Dy2
TCTPR-9	D_{3h}	Tricapped trigonal prism	22.597
JTDIC-9	C_{3v}	Tridiminished icosahedron J63	28.559
HH-9	C_{2v}	Hula-hoop	27.147
MFF-9	C_s	Muffin	22.025
EP-9	D_{9h}	Enneagon	47.343
OPY-9	C_{8v}	Octagonal pyramid	40.127
HBPY-9	D_{7h}	Heptagonal bipyramid	34.360
JTC-9	C_{3v}	Triangular cupola J3	31.131
JCCU-9	C_{4v}	Capped cube (J8)	30.857
CCU-9	C_4	Capped cube	29.668
JCSAPR-9	C_{4v}	Capped sq. antiprism	26.540
CSAPR-9	C_{4v}	Capped square antiprism	25.299
JTCTPR-9	D_{3h}	Tricapped trigonal prism J51	28.299
TCTPR-9	D_{3h}	Tricapped trigonal prism	25.961
JTDIC-9	C_{3v}	Tridiminished icosahedron J63	33.532
HH-9	C_{2v}	Hula-hoop	28.400
MFF-9	C_s	Muffin	25.092

Table 6. The parameters XT, XS, alpha and tau.

Cluster **1**			
ChiS	ChiT	Tau	Alpha
8.67134	49.5211	1.80549E-4	0.1738
10.2243	39.684	1.53988E-4	0.12952
7.90081	33.0114	1.02608E-4	0.14413
7.80415	28.132	8.06073E-5	0.13825
7.43727	24.4497	6.15848E-5	0.14091
5.49536	21.5628	3.9337E-5	0.15687
2.59512	19.2577	2.20995E-5	0.17878
1.85508E-12	17.3831	1.23094E-5	0.2015
1.78953E-12	15.8167	8.67187E-6	0.21673
3.20567E-12	14.5003	6.27742E-6	0.23413
3.27229E-12	13.3821	4.75857E-6	0.2512
Cluster **2**			
15.7664	33.9937	2.86092E-4	0.21657
15.1426	31.8292	2.70699E-4	0.21383
14.606	29.8411	2.59686E-4	0.20816
14.0686	28.0465	2.49847E-4	0.20308
13.5273	26.435	2.40314E-4	0.19918
13.0457	24.9662	2.31672E-4	0.19293
12.3109	22.8191	2.17056E-4	0.18158
11.6189	21.0041	1.99881E-4	0.16991

11.0506	19.4284	1.82495E-4	0.15159
10.4974	18.0691	1.62795E-4	0.13447
10.0028	16.8865	1.43237E-4	0.1178
9.4813	15.8422	1.22721E-4	0.10281
9.0076	14.9234	1.04473E-4	0.09009
8.46449	14.1082	8.60956E-5	0.08363
8.00792	13.3766	7.1863E-5	0.07416
7.50159	12.7158	5.845E-5	0.06801
Cluster **3**			
54.9109	56.6814	4.75602E-4	2.1474E-9
47.5281	48.4221	5.27037E-4	5.94288E-9
41.8593	42.2959	6.87485E-4	5.41767E-9
37.4664	37.647	0.00103	6.97224E-9
33.9507	34.028	0.00161	9.42801E-9
31.1061	31.0603	0.00354	2.86696E-21
28.7367	28.6471	0.1041	5.75196E-20
26.7509	26.6749	0.04078	1.01317E-19
25.0608	25.0052	0.02888	1.45199E-19
23.6114	23.6114	0.02489	1.99487E-19
22.3436	22.2941	0.01976	2.6478E-19
21.2341	21.1888	0.02323	3.00671E-19
20.2461	20.1851	0.03368	1.86315E-19
19.3579	19.3243	0.06421	1.23708E-19

Note 1

SQUEEZE and "Use Solvent Mask results" results for cluster **1-3** are as follows:

(1) Cluster 1

```
 loop_
_platon_squeeze_void_nr
_platon_squeeze_void_average_x
_platon_squeeze_void_average_y
_platon_squeeze_void_average_z
_platon_squeeze_void_volume
_platon_squeeze_void_count_electrons
_platon_squeeze_void_content
1 0.000 0.000 0.000 872 244 "
```

A solvent mask was calculated, and 244 electrons were found in a volume of 872 $Å^3$ in 1 void per unit cell. This is consistent with the presence of 1[C_2H_3N], 10[H_2O] per Asymmetric Unit which account for 244 electrons per unit cell. Further combined with elemental analysis and thermogravimetric analysis results (Figure S2), the molecular formula of cluster **1** is calculated to be [$Dy_5(HL^1)_2(L^1)_4(\mu_3\text{-}OH)_2(NO_3)_3$]·$2CH_3CN$·$10H_2O$

(2) Cluster 2

loop_
   _smtbx_masks_void_nr
   _smtbx_masks_void_average_x
   _smtbx_masks_void_average_y
   _smtbx_masks_void_average_z
   _smtbx_masks_void_volume
   _smtbx_masks_void_count_electrons
   _smtbx_masks_void_content
   1 0.491 0.000 0.500 611.3 145.3 '0.5 12[CH₃CN]2[H₂O]'
   2 0.032 0.500 0.000 611.3 145.3 '0.5 12[CH₃CN]2[H₂O]'

Further combined with elemental analysis and thermogravimetric analysis results (Figure S2), the molecular formula of cluster **2** is calculated to be $[Dy_8(HL^2)_6(\mu_3\text{-OH})_4(\mu_2\text{-OH})_2(NO_3)_4(OCH_3)_2(H_2O)_2]\cdot6CH_3CN\cdot H_2O$

(3) Cluster 3

loop_
   _platon_squeeze_void_nr
   _platon_squeeze_void_average_x
   _platon_squeeze_void_average_y
   _platon_squeeze_void_average_z
   _platon_squeeze_void_volume
   _platon_squeeze_void_count_electrons
   _platon_squeeze_void_content
   1 0.441 0.087 -0.048 10066 2912 ' '92 MeCN,92 H₂O'
   2 0.000 0.000 0.000 421 77 ' '2 MeCN, 2 H₂O'
   3 0.899 0.178 0.765 9 -1 ' '
   4 0.399 0.322 0.265 10 -1 ' '
   5 0.500 0.500 0.500 421 77 ' '2 MeCN, 2 H₂O'
   6 0.601 0.678 0.735 9 -1 ' '
   7 0.101 0.822 0.235 9 -1 ' '

A solvent mask was calculated and 3063 electrons were found in a volume of 10935\%A^3^ in 3 voids per unit cell. This is consistent with the presence of 23[C₂H₃N], 23[H₂O], 1[C₂H₃N], 1[H₂O], per Asymmetric Unit which account for 3072 electrons per unit cell. Therefore，the molecular formula of cluster **3** is calculated to be $[Dy_{14}(HL^3)_7(OAc)_{28}]\cdot24CH_3CN\cdot31H_2O$.